

Large Magnetoresistance and Weak Antilocalization Effect in $\text{Bi}_2\text{Se}_{2.1}\text{Te}_{0.9}$ Topological Single Crystal

K. Shrestha^{1*} and D. E. Graf², V. Marinova³, B. Lorenz⁴ and C. W. Chu^{4,5}

¹*Idaho National Laboratory, 2525 Fremont Ave, Idaho Falls, ID 83401, USA*

²*National High Magnetic Field Laboratory, Florida State University, Tallahassee, Florida 32306-4005, USA*

³*Institute of Optical Materials and Technology, Bulgarian Academy of Sciences, Acad. G. Bontchev Street 109, Sofia 1113, Bulgaria*

⁴*TCSUH and Department of Physics, University of Houston, 3201 Cullen Boulevard, Houston, Texas 77204, USA and*

⁵*Lawrence Berkeley National Laboratory, 1 Cyclotron Road, Berkeley, California 94720, USA*

We have investigated the weak antilocalization (WAL) effect in our previously studied p -type $\text{Bi}_2\text{Se}_{2.1}\text{Te}_{0.9}$ topological system [PRB **90**, 241111(R)(2014) and Phil. Mag. **97**, 1740 (2017)]. The magnetoconductance shows a cusp-like feature at low magnetic fields, indicating the presence of the WAL effect. The WAL curves measured at different tilt angles merge together when they are plotted as a function of the normal field components, showing that surface states dominate the magnetoconductance in the $\text{Bi}_2\text{Se}_{2.1}\text{Te}_{0.9}$ crystal. Several physical parameters that characterize the WAL effect were determined using the Hikami-Larkin-Nagaoka formula and their temperature dependence was studied from 0.33 K up to 20 K. Nearly constant values of phase coherence length and the number of conduction channels with temperature implies that the system is robust up to 20 K. In addition, the sample shows a large positive magnetoresistance that reaches 1900% under magnetic fields of 35 T at $T=0.33$ K with no sign of saturation. The magnetoresistance value decreases with both increasing temperature and tilt angle of the sample surface with respect to the magnetic field. The large magnetoresistance of topological insulators can be utilized in future technology such as sensors and memory devices.

I. INTRODUCTION

Three-dimensional topological insulators (TIs) have attracted significant attention as they possess topologically protected metallic states on their surfaces, known as surface states^{1,2,3,4,5}. These metallic surface states in 3D TIs originate as a result of the nontrivial topology of the bulk band structure and are protected by time-reversal symmetry. Due to the topological protection of these metallic states, surface-state electrons have very high mobility and are less sensitive to impurities (if the impurity is not magnetic). Recently, very large magnetoresistance and high mobility have also been observed in many topological systems^{6,7}, making TIs not only a playground for understanding novel quantum phenomena but promising candidates for future electronic devices as well. Many bismuth-based TIs have been theoretically predicted and have later been experimentally verified by surface-sensitive techniques such as angle-resolved photoelectron spectroscopy and scanning electron microscopy^{8,9,10}. Electrical transport (or magnetization) measurements under high magnetic fields have often been used to study topological systems. In the presence of magnetic fields, electrical conductivity (or magnetization) shows quantum oscillations known as Shubnikov de Haas (de Haas van Alphen) effects^{11,12,13}. By analyzing oscillations at different tilt angles of the sample with respect to magnetic fields, one can map the two-dimensional Fermi surface of surface states or the three-dimensional Fermi surface of bulk states and thus study many additional properties^{7,14}. However, transport studies of surface states in 3D TIs are always hin-

dered due to the presence of the parallel bulk conduction channel that arises as a result of crystal defects and imperfections^{15,16,17,18}. Several efforts have been made to grow purer topological crystals by modifying the crystal growth technique, compensating excess bulk carriers by doping Sb or Ca ions, and extending research from binary to ternary topological compounds^{19,20,21,22,23,24}.

In our recent magnetotransport studies^{25,26} on metallic $\text{Bi}_2\text{Se}_{2.1}\text{Te}_{0.9}$ single crystals, we have observed well separated signals from the surface and bulk states. The surface states dominate at low fields (below 7 T) and bulk states at high fields. The crossover between these signals takes place at 14 T. These results have shown that it may be possible to characterize surface-state properties even if the bulk is metallic.

Due to the presence of strong spin-orbit coupling in topological materials, their magnetoconductance often shows a weak antilocalization (WAL) effect^{27,28}. As a quantum correction to a classical conductance, a WAL effect in topological insulators may originate due to spin-orbit coupling in either the surface or bulk states. Whether the WAL effect originates from surface or bulk states can be determined by measuring the magnetoconductance at different angles between the sample and the magnetic field direction. Recently, numerous topological systems have been successfully investigated by means of the WAL effect^{19,29} where physical properties, such as the phase coherence length and the number of conduction channels, were determined; such measurements are not possible using the quantum oscillations method. It would therefore be interesting to extend the study of the $\text{Bi}_2\text{Se}_{2.1}\text{Te}_{0.9}$ sample by the WAL method.

In this work, we have carried out magnetoresistance studies on a $\text{Bi}_2\text{Se}_{2.1}\text{Te}_{0.9}$ single crystal under high magnetic fields up to 35 T. The sample shows a large non-saturating magnetoresistance that reaches 1900% at $T=0.33$ K. Magnetoconductance in low magnetic fields shows a cusp due to the WAL effect. From the angle dependence of the WAL curves, we prove the presence of topological surface states in a $\text{Bi}_2\text{Se}_{2.1}\text{Te}_{0.9}$ single crystal. We have estimated several physical parameters using the Hikami-Larkin-Nagaoka formula and have studied their temperature dependence as well.

II. EXPERIMENTAL DETAILS

High-quality $\text{Bi}_2\text{Se}_{2.1}\text{Te}_{0.9}$ single crystals were grown using the modified Bridgman method. Stoichiometric amounts of high purity Bi (99.9999%), Se (99.9999%), and Te (99.9999%) were mixed together and enclosed in quartz ampoules. The mixture melts at 875 °C and was kept at this temperature for 2 days. The molten mixture was slowly cooled to 670 °C at a rate of 0.5 °C/h and then to room temperature at a rate of 10 °C/h. A shiny plate-like single crystal was selected from the boules of crystals and six gold contact pads were sputtered as shown in the lower inset to Fig. [1]. Dimensions of the single crystal are 3 mm x 2 mm x 0.1 mm. Five platinum wires were attached to these gold contact pads using silver paint to carry out the standard longitudinal and Hall measurements. To ensure safe handling of the sample, it was attached to a magnesium oxide (MgO) substrate using GE varnish.

Transport measurements of the $\text{Bi}_2\text{Se}_{2.1}\text{Te}_{0.9}$ single crystal under magnetic fields up to 7 T were performed in a Physical Properties Measurement System (PPMS) at the Texas Center for Superconductivity at the University of Houston. The field range was extended to 35 T by performing measurements at the National High Magnetic Field Laboratory (NHMFL), Tallahassee, Florida. The angle-dependence measurements were carried out by mounting the sample on a rotating platform on a standard probe designed at NHMFL. Longitudinal and Hall resistances were measured using a lock-in technique in which a Keithley (6221) source meter provides AC current of amplitude 1 mA at a certain frequency, 47.77 Hz and the lock-in amplifier (SR-830) measures the voltage signal at the same frequency. The standard probe with the sample mounted on it was inserted into a ^3He Oxford cryostat that sits into the bore of a resistive magnet with a maximum field of 35 T. A Hall sensor was used to calibrate the position of the sample with respect to the direction of the applied field.

III. RESULTS AND DISCUSSION

Figure [1] shows the temperature dependence of longitudinal resistance of a $\text{Bi}_2\text{Se}_{2.1}\text{Te}_{0.9}$ single crystal. The

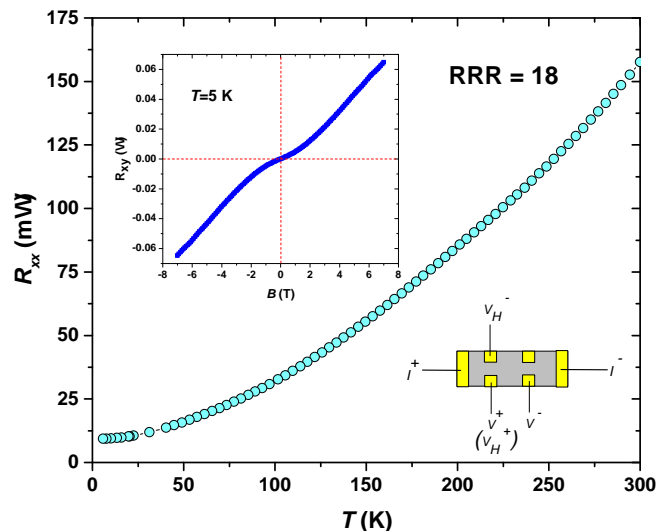


FIG. 1. Temperature dependence of longitudinal resistance of a $\text{Bi}_2\text{Se}_{2.1}\text{Te}_{0.9}$ single crystal. Upper inset: Hall measurement data of $\text{Bi}_2\text{Se}_{2.1}\text{Te}_{0.9}$ at $T=5$ K. Lower inset: schematic diagram of the sample configuration for longitudinal and Hall measurements. Yellow patches show gold contact pads sputtered on the sample surface.

sample shows a metallic behavior from 300 to 5 K. The high value of the residual resistance ratio, $\text{RRR} = R_{xx}(300 \text{ K})/R_{xx}(5 \text{ K}) = 18$ indicates good crystalline quality. This RRR value is comparable with those of $\text{Bi}_2\text{Se}_{2.1}\text{Te}_{0.9}$ single crystals used in our previous studies^{25,26}. The upper inset shows Hall measurements at $T=5$ K. The positive slope of the Hall resistance reveals the presence of hole-like bulk charge carriers. The Hall resistance shows the non-linear behavior near the origin, $B=0$, indicating the presence of multiband effects (hole and electron bands), as has been observed in other bismuth-based topological systems^{15,25}. From the slope of the Hall data, we have estimated the bulk carrier concentration to be $\approx 7 \times 10^{18} \text{cm}^{-3}$ at 5 K.

The magnetoresistance of a $\text{Bi}_2\text{Se}_{2.1}\text{Te}_{0.9}$ single crystal was measured under high magnetic fields up to 35 T at NHMFL. The raw magnetoresistance data measured at angle $\theta=0^\circ$ is shown in the inset to Fig.[2(a)]. Here, the angle θ is defined as the angle between the magnetic field direction and the perpendicular to the sample surface, as shown in the inset to Fig. [2(c)]. The magnetoresistance is anisotropic with field direction which could be due to the geometry of contacts; however, the transverse component can be removed by taking an average of magnetoresistance values in positive and negative field directions, i.e., $[R_{xx}(B) + R_{xx}(-B)]/2$. Figure [2(a)] shows the symmetrized magnetoresistance of $\text{Bi}_2\text{Se}_{2.1}\text{Te}_{0.9}$ expressed as a percentage, $\text{MR} = [R_{xx}(B)/R_{xx}(0) - 1] \times 100\%$, where $R_{xx}(0)$ and $R_{xx}(B)$ are resistances at zero and B applied field, respectively. The sample shows a large positive MR that reaches up to 2000% under magnetic fields of 35 T at $\theta=0^\circ$ and it continues to increase linearly with field.

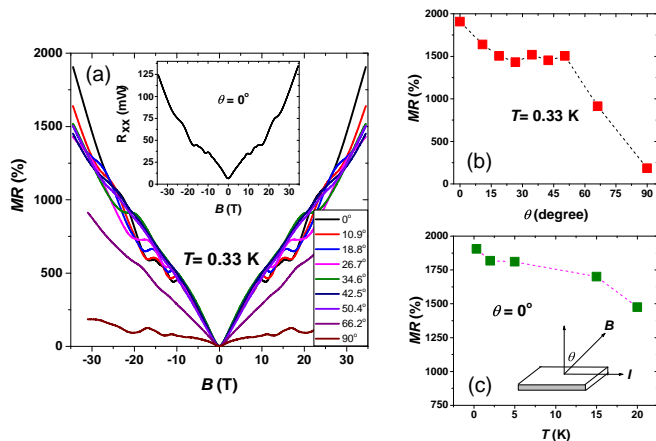


FIG. 2. (a) Angle dependence of MR of a $\text{Bi}_2\text{Se}_{2.1}\text{Te}_{0.9}$ single crystal expressed as a percentage in magnetic fields up to 34.5 T at $T=0.33$ K. (b) MR value at highest magnetic field as a function of tilt angle, θ , at $T=0.33$ K. (c) MR value at highest magnetic field at different temperatures measured at $\theta=0^\circ$. Inset: θ is the angle between magnetic field and normal to the sample surface.

This MR value is comparable with those of other topological systems^{25,26}. The presence of the sharp cusp-like feature in MR indicates the weak antilocalization effect (WAL) in the $\text{Bi}_2\text{Se}_{2.1}\text{Te}_{0.9}$ sample, which we will discuss later in detail. It should be noted that MR shows clear quantum oscillations in fields above 10 T. The oscillations have two frequencies at $F_1 \approx 26$ T and $F_2 \approx 55$ T in the frequency spectrum. From the angle dependence of F_1 and F_2 and Berry phase calculations, we have already resolved the origin of these frequencies in our previous studies^{25,26}. The MR value strongly depends on the θ value. Fig.[2(b)] shows the variation of MR values with θ . MR is maximum at $\theta=0^\circ$, and it decreases gradually up to 50.4° and then rapidly with a further increase in θ . At $\theta=60.2^\circ$, MR reaches 1000% at 35 T, which is almost $\frac{1}{2}$ of the value at $\theta=0^\circ$. Similarly, the MR value decreases with increasing temperature, as shown in Fig. [2(c)]. At $T=20$ K, $\text{MR}=1475\%$, which is almost $\frac{2}{3}$ of the MR value at $T=0.33$ K.

In order to investigate the origin of the WAL effect in the $\text{Bi}_2\text{Se}_{2.1}\text{Te}_{0.9}$ single crystal, we have studied magnetoconductance at different tilt angles, θ . The WAL-induced quantum corrections to magnetoconductance can be obtained as²⁷

$$\Delta G(\theta, B) = 1/R_{xx}(\theta, B) - 1/R_{xx}(\theta = 90^\circ, B), \quad (1)$$

where $R_{xx}(\theta, B)$ and $R_{xx}(\theta = 90^\circ, B)$ are magnetoresistance at a given θ value and at $\theta=90^\circ$, respectively. Figure [3(a)] shows $\Delta G(\theta, B)$ of the $\text{Bi}_2\text{Se}_{2.1}\text{Te}_{0.9}$ crystal measured along different tilt angles at $T=0.33$ K. Magnetoconductance shows a strong dependence on the θ values. All of the magnetoconductance curves merge together when they are plotted as a function of the normal

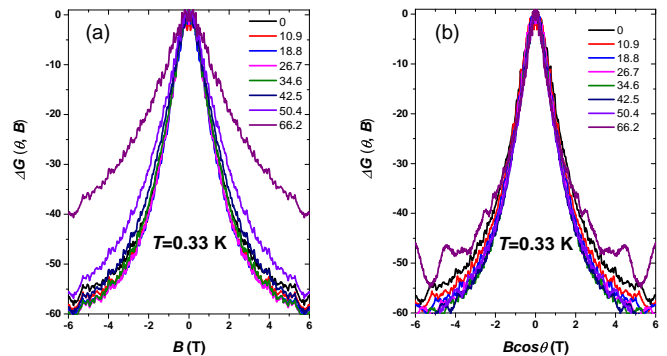


FIG. 3. Magnetoconductance curves of $\text{Bi}_2\text{Se}_{2.1}\text{Te}_{0.9}$ single crystal as a function of (a) B and (b) $B\cos\theta$ under fields up to 6 T at $T=0.33$ K.

component of magnetic fields, $B\cos\theta$, as shown in Fig. [3(b)]. This provides strong evidence of the dominance of topological surface states in the magnetoconductance of the $\text{Bi}_2\text{Se}_{2.1}\text{Te}_{0.9}$ single crystal. This observation is consistent with the previous conclusions at low magnetic fields^{25,26}.

We have used the Hikami-Larkin-Nagaoka (HLN) formula to determine various physical parameters that characterize the WAL effect in the $\text{Bi}_2\text{Se}_{2.1}\text{Te}_{0.9}$ single crystal. According to the HLN formula³⁰, magnetoconductance can be described as,

$$\Delta G(\theta = 0, B) = A \left[\Psi \left(\frac{1}{2} + \frac{\hbar}{4eL_\phi^2 B} \right) - \ln \left(\frac{\hbar}{4eL_\phi^2} \right) \right]. \quad (2)$$

Here Ψ is the digamma function, and L_ϕ is the phase coherence length, which is the distance traveled by an electron before its phase is changed. The parameter $A = \alpha \frac{e^2}{2\pi^2 \hbar}$ with $\alpha=1/2$ per conduction channel. Thus, A represents the number of conduction channels present in a sample. Using equation (2) with our experimental data, the fitting parameters L_ϕ and A can be determined. Figure [4(a)] shows the magnetoconductance data at $T=0.33$ K in a low field range (-2 to 2 T). The magnetoconductivity data is well described by the HLN formula as shown by the dashed curve. The fitting yields $L_\phi=25.5$ nm and $A=62.5 \Omega^{-1}$ at $T=0.33$ K. These values are comparable to those of previously reported data for other topological systems^{31,32}. In order to explore the robustness of system in terms of conduction, we have calculated the parameters, L_ϕ and A at different temperatures as shown in Fig. [4(b, c)]. The phase coherence length shows a very weak dependence on temperature up to 20 K. Similarly, A remains almost independent of temperature up to 20 K, indicating the presence of a fixed number of conduction channels in the $\text{Bi}_2\text{Se}_{2.1}\text{Te}_{0.9}$ single crystal. This means that the system is sturdy in temperatures up to 20 K.

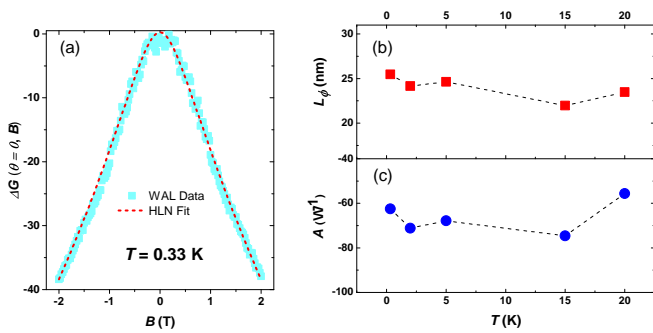


FIG. 4. (a) Magnetoconductance curve of $\text{Bi}_2\text{Se}_{2.1}\text{Te}_{0.9}$ single crystal within (-2 to 2 T) field range at $\theta=0^\circ$. The dashed curve shows the best fit curve obtained by using the HLN formula. (b, c) Temperature dependence of phase coherence length l_ϕ and pre-factor A , respectively.

IV. SUMMARY

In summary, we have carried out magnetotransport studies on the $\text{Bi}_2\text{Se}_{2.1}\text{Te}_{0.9}$ single crystal under fields up to 35 T. The resistance and Hall measurements show that $\text{Bi}_2\text{Se}_{2.1}\text{Te}_{0.9}$ is metallic below room temperature with hole-like bulk charge carriers. Under magnetic field measurements, the sample shows a large positive magnetoresistance that reaches as high as 1900% without any sign of saturation up to 35 T. Magnetoresistance decreases with increasing temperature and tilt angle of

the sample with respect to magnetic fields. In addition, the magnetoresistance has a sharp cusp-like feature, indicating the presence of the weak antilocalization (WAL) effect. The magnetoconductance curves vary with the normal components of magnetic fields, confirming the presence of topological surface states in $\text{Bi}_2\text{Se}_{2.1}\text{Te}_{0.9}$. We have used the Hikami-Larkin-Nagaoka formula to estimate different physical parameters that characterize the WAL effect. Nearly constant values of the phase coherence length and the number of conduction channels imply that the system is robust in temperature up to 20 K.

ACKNOWLEDGEMENTS

This work is supported in part by the U.S. Air Force Office of Scientific Research Grant FA9550-15-1-0236, the T. L. L. Temple Foundation, the John J. and Rebecca Moores Endowment, and the State of Texas through the Texas Center for Superconductivity at the University of Houston. V. Marinova acknowledges support from the Bulgarian Science Fund project DN 08/9. A portion of this work was performed at the National High Magnetic Field Laboratory, which is supported by National Science Foundation Cooperative Agreement No. DMR-1157490 and the State of Florida. The work at Idaho National Laboratory is supported by Department of Energy, Office of Basic Energy Sciences, Materials Sciences, and Engineering Division.

* Corresponding E-mail: keshav.shrestha@inl.gov

¹ M. Z. Hasan and C. L. Kane, *Rev. Mod. Phys.* **82**, 3045 (2010).

² X. L. Qi and S.-C. Zhang, *Rev. Mod. Phys.* **83**, 1057 (2011).

³ Y. Ando, *J. Phys. Soc. Jpn.* **82**, 102001 (2013).

⁴ Y. Ando and L. Fu, *Annu. Rev. Condens. Matter Phys.* **6**, 361 (2015).

⁵ R. J. Cava, H. Ji, M. K. Fuccillo, Q. D. Gibson, and Y. S. Hor, *J. Mater. Chem. C* **1**, 3176 (2013).

⁶ K. Shrestha, M. Chou, D. Graf, H. D. Yang, B. Lorenz, and C. W. Chu, *Phys. Rev. B* **95**, 195113 (2017).

⁷ X. Wang, Y. Du, S. Dou, and C. Zhang, *Phys. Rev. Lett.* **108**, 266806 (2012).

⁸ Y. Xia, D. Qian, D. Hsieh, L. Wray, A. Pal, H. Lin, A. Bansil, D. Grauer, Y. S. Hor, R. J. Cava, and M. Z. Hasan, *Nat. Phys.* **5**, 398 (2009).

⁹ Y. L. Chen, J. G. Analytis, J.-H. Chu, Z. K. Liu, S.-K. Mo, X. L. Qi, H. J. Zhang, D. H. Lu, X. Dai, Z. Fang, S. C. Zhang, I. R. Fisher, Z. Hussain, and Z.-X. Shen, *Science* **325**, 178 (2009).

¹⁰ D. Hsieh, Y. Xia, D. Qian, L. Wray, F. Meier, J. H. Dil, J. Osterwalder, L. Patthey, A. V. Fedorov, H. Lin, A. Bansil, D. Grauer, Y. S. Hor, R. J. Cava, and M. Z. Hasan, *Phys. Rev. Lett* **103**, 146401 (2009).

¹¹ C. Kittel, *Introduction to Solid State Physics*, Vol. (Pushp Print Service, Delhi, 2006).

¹² Ashcroft and Mermin, *Solid State Physics*, Vol. (Holt, Rinehart and Winston, New York, 1976).

¹³ D. Shoenberg, *Magnetic Oscillations in Metals* (Cambridge University Press, 1984).

¹⁴ K. Shrestha, V. Marinova, D. Graf, B. Lorenz, and C. W. Chu, *Phys. Rev. B* **95**, 075102 (2017).

¹⁵ D.-X. Qu, Y. S. Hor, J. Xiong, R. J. Cava, and N. P. Ong, *Science* **329**, 821 (2010).

¹⁶ J. G. Analytis, R. D. McDonald, S. C. Riggs, J.-H. Chu, G. S. Boebinger, and I. R. Fisher, *Nat. Phys.* **6**, 960 (2010).

¹⁷ K. Eto, Z. Ren, A. A. Taskin, K. Segawa, and Y. Ando, *Phys. Rev. B* **81**, 195309 (2010).

¹⁸ H. Cao, S. Xu, I. Miotkowski, J. Tian, D. Pandey, M. Z. Hasan, and Y. P. Chen, *Phys. Status Solidi RRL* **7**, 133 (2013).

¹⁹ A. A. Taskin, Z. Ren, S. Sasaki, K. Segawa, and Y. Ando, *Phys. Rev. Lett.* **107**, 016801 (2011).

²⁰ G. Eguchi, K. Kuroda, K. Shirai, A. Kimura, and M. Shiraishi, *Phys. Rev. B* **90**, 201307 (2014).

²¹ Y. S. Hor, A. Richardella, P. Roushan, Y. Xia, J. G. Checkelsky, A. Yazdani, M. Z. Hasan, N. P. Ong, and R. J. Cava, *Phys. Rev. B* **79**, 195208 (2009).

- ²² L. Bao, L. He, N. Meyer, X. Kou, P. Zhang, Z. G. Chen, A. V. Fedorov, J. Zou, T. M. Riedemann, T. A. Lograsso, K. L. Wang, G. Tuttle, and F. Xiu, *Nat. Sci. Rep.* **2**, 726 (2012).
- ²³ S.-Y. Xu, L. A. Wray, Y. Xia, R. Shankar, A. Petersen, A. Fedorov, H. Lin, A. Bansil, Y. S. Hor, D. Grauer, R. J. Cava, and M. Z. Hasan, *arXiv Cond. Mat.* 1007.5111, unpublished.
- ²⁴ H. Lin, T. Das, L. A. Wray, S.-Y. Xu, M. Z. Hasan, and A. Bansil, *New Jour. Phys.* **13**, 095005 (2011).
- ²⁵ K. Shrestha, V. Marinova, B. Lorenz, and P. C. W. Chu, *Phys. Rev. B* **90**, 241111 (2014).
- ²⁶ K. Shrestha, D. E. Graf, V. Marinova, B. Lorenz, and P. C. W. Chu, *Philosophical Magazine* **97**, 1740 (2017).
- ²⁷ H. T. He, G. Wang, T. Zhang, I. K. Sou, G. K. L. Wong, J. N. Wang, H. Z. Lu, S. Q. Shen, and F. C. Zhang, *Phys. Rev. Lett.* **106**, 166805 (2011).
- ²⁸ K. Shrestha, V. Marinova, D. E. Graf, B. Lorenz, and C. W. Chu, *arXiv:1704.02682*.
- ²⁹ C. Shekhar, C. E. ViolaBarbosa, B. Yan, S. Quardi, W. Schnelle, G. H. Fecher, and C. Felser, *Phys. Rev. B* **90**, 165140 (2014).
- ³⁰ S. Hikami, A. I. Larkin, and Y. Nagaoka, *Progress of Theoretical Physics* **63**, 707 (1980).
- ³¹ G. Xu, W. Wang, X. Zhang, Y. Du, E. Liu, S. Wang, G. Wu, Z. Liu, and X. X. Zhang, *Nat. Sci. Rep.* **4**, 5709 (2014).
- ³² J. G. Checkelsky, Y. S. Hor, M. H. Liu, D. X. Qu, R. J. Cava, and N. P. Ong, *Phys. Rev. Lett.* **103**, 246601 (2009).